







Featured Article

Ankylosaurian body armor function and evolution with insights from osteohistology and morphometrics of new specimens from the Late Cretaceous of Antarctica

Arthur S. Brum* , Lúcia H. S. Eleutério, Tiago R. Simões* , Megan R. Whitney ,
Geovane A. Souza , Juliana M. Sayão , and Alexander W. A. Kellner 

Abstract.—The body armor of ankylosaurians is a unique morphological feature among dinosaurs. While ankylosaurian body armor has been studied for decades, paleohistological analyses have only started to uncover the details of its function. Yet there has been an overall bias toward sampling ankylosaurian remains from the Northern Hemisphere, with limited quantitative studies on the morphological and functional evolution of the osteoderms composing their body armor. Here, we describe new ankylosaurian materials recovered from the Late Cretaceous of Antarctica that, in combination with data compiled from the literature, reveal new insights into the evolution of the ankylosaurian body armor. Based on histological microstructure and phylogenetic results, the new Antarctic material can be assigned to Nodosauridae. This group shares the absence/poor development of their osteodermal basal cortex and highly ordered sets of orthogonal structural fibers in the superficial cortex. Our morphospace analyses indicate that large morphological diversity is observed among both nodosaurids and ankylosaurids, but osteoderms became more functionally specialized in late-diverging nodosaurids. Besides acting as effective protection against predation, osteoderms also exhibit highly ordered structural fibers in nodosaurids, enabling a decrease in cortical bone thickness (as in titanosaurs), which could have been co-opted for secondary functions, such as calcium remobilization for physiological balance. The latter may have played a key role in nodosaurid colonization of high-latitude environments, such as Antarctica and the Arctic Circle.

Arthur S. Brum, Geovane A. Souza, and Juliana M. Sayão. Laboratório de Paleobiologia e Paleogeografia Antártica, Departamento de Geologia e Paleontologia, Museu Nacional-Universidade Federal do Rio de Janeiro, Quinta da Boa Vista, São Cristóvão, Rio de Janeiro, Rio de Janeiro 20940-040, Brazil. E-mail: arthursbc@yahoo.com.br, geosoouza@gmail.com, jmsayao@mn.ufrj.br

Lúcia H. S. Eleutério. Laboratório de Paleobiologia e Microestruturas, Centro Acadêmico de Vitória, UFPE, Alto do Reservatório, s/n, Vitória de Santo Antão, Pernambuco 55608-680, Brazil. E-mail: luciahelenaeb@gmail.com

Tiago R. Simões. Department of Organismic & Evolutionary Biology, Museum of Comparative Zoology, Harvard University, Cambridge, Massachusetts 02138, U.S.A. E-mail: tsimoes@fas.harvard.edu

Megan R. Whitney. Department of Biology, Loyola University of Chicago, Chicago, Illinois 60660, U.S.A. E-mail: mwhitney@luc.edu

Alexander W. A. Kellner. LAPUG, Departamento de Geologia e Paleontologia, Museu Nacional/Universidade Federal do Rio de Janeiro, Quinta da Boa Vista s/n, São Cristóvão, Rio de Janeiro, Rio de Janeiro 20940-040, Brazil. E-mail: kellner@mn.ufrj.br

Accepted: 17 January 2023

*Corresponding author.

Introduction

Ankylosaurian dinosaurs are one of the most peculiar groups of reptiles in the fossil record due to their extensive body covering of osteoderms creating a massive body armor that is unlike any other in the evolution of dinosaurs (e.g., Kirkland et al. 2013; Brown et al. 2017). Osteoderm size and shape are diverse among

ankylosaurian groups and even across distinct body regions within the same individual (e.g., tail knobs, ossicles, spines, and thoracic osteoderms; Brown et al. 2017). However, the usage of osteoderm features to better understand ankylosaurian phylogeny and evolutionary patterns is still in its infancy. For instance, using osteoderm characters for phylogenetic reconstructions of ankylosaur phylogeny is



relatively recent (Hill 2005; Burns and Currie 2014; Arbour and Currie 2016; Soto-Acuña et al. 2021). In studies of osteoderm variation among distinct ankylosaurian groups, paleohistological analyses indicate some major differences in microstructure patterns (Scheyer and Sander 2004; Hayashi et al. 2010; Burns and Currie 2014). However, such differences have rarely been investigated in a macroevolutionary context using quantitative methods.

Additionally, the ankylosaurian fossil record is marked by major geographic sampling discrepancies, such as the larger sampling of ankylosaurians in the Northern Hemisphere compared with the southern continents (Arbour and Currie 2016; Arbour et al. 2016). This biogeographic sampling discrepancy inherently limits the taxonomic and morphological information available on this group on a global scale, which may impact our understanding of their taxonomic and morphological diversity, as shown by recent discoveries (e.g., Maidment et al. 2021; Soto-Acuña et al. 2021; Frauenfelder et al. 2022). Therefore, further sampling of ankylosaur remains from continents derived from Gondwana is critical to better understand their evolutionary trajectories.

The Antarctic continent is the most underexplored frontier of paleontology in the Southern Hemisphere (and perhaps globally). Antarctica represents a significant portion of all landmasses in the Southern Hemisphere, but only very few regions have exposed sedimentary outcrops that can provide insights into the evolution of life on Earth (e.g., Olivero 2012b; Burton-Johnson and Riley 2015; Piovesan et al. 2021). Despite such limitations, several vertebrate remains have been discovered in Antarctica over the past few decades. These discoveries include plesiosaurs (e.g., O’Gorman et al. 2019; Brum et al. 2022), pterosaurs (Kellner et al. 2019), and dinosaurs (Lamanna et al. 2019); for an updated survey of fossil vertebrates in the Upper Cretaceous of Antarctica, see Reguero et al. (2022). Importantly, this includes one ankylosaurian species, *Antarctopelta oliveroi* Salgado and Gasparini, 2006—although there is some dispute on the validity of this taxon (Arbour and Currie 2016; Rozadilla et al. 2016).

Since 2007, the project PALEOANTAR (organized by the Museu Nacional/Universidade

Federal do Rio de Janeiro, Brazil) has been working in the Antarctic Peninsula to shed light on the diversification and evolutionary history of Antarctic ecosystems in the deep past (Lima et al. 2021; Kellner 2022; Santos et al. 2022), including studies on Mesozoic vertebrates (e.g., Kellner et al. 2011, 2019; Brum et al. 2022) and invertebrates (e.g., Pinheiro et al. 2020; Videira-Santos 2020; Piovesan et al. 2021). Here, we report on new ankylosaurian materials recovered from Antarctica during the PALEOANTAR expedition in 2015. The material consists of ankylosaurian osteoderms found on Santa Marta Cove, James Ross Island (James Ross Basin, Antarctic Peninsula), which come from the same levels where *Antarctopelta* was previously found. Combining paleohistological, phylogenetic, and morphometric approaches, we assign these new specimens to late-diverging nodosaurids, thus expanding the phylogenetic diversity of Antarctic ankylosaurians. Further, we compiled osteoderm data from the literature that—combined with the new materials described here—provide the first detailed quantitative analysis of the evolution of the ankylosaurian body armor microstructure. We show that late-diverging nodosaurids (including our new specimens) expanded ankylosaur morphospace by decreasing the cortical thickness, which may be associated with a structural shift in their osteoderms by a major structural fiber rearrangement. We also indicate that the expansion of the core and its vascularization in late-diverging nodosaurids is similar to that observed in some titanosaurs, suggesting both an effective body armor function and a co-opted function of calcium remobilization for physiological balance. Such plastic physiology may have played a key role in the dispersal potential of this group toward higher latitudes, which present a greater disparity of climatic conditions throughout the year compared with lower latitudes.

Materials and Methods

Materials

The new specimens reported here were collected on James Ross Island and comprise three isolated osteoderms (CAV-A4, CAV-A5,

and CAV-A10). The specimens and paleohistological slides are housed in the Laboratório de Paleobiologia e Microestruturas, Centro Acadêmico de Vitória, Universidade Federal de Pernambuco (Vitória de Santo Antão, State of Pernambuco, Brazil—CAV).

Anatomical Terminology

We followed the terminology of Scheyer and Sander (2004) and Burns and Currie (2014) to describe the anatomical osteoderm orientation, in which the core is the internal cancellous region (Burns and Currie 2014; Fig. 1), while the cortex comprises the basal (toward the internal region of the bone) and superficial layers of compact bone (or external, toward the surface of the bone; Scheyer and Sander 2004). The core could be filled by cancellous bone, with a high density of resorption cavities, or be more compacted. The cortex comprises bone that is more compact and, in some cases, exhibits a decrease in vascularization. The microstructural nomenclature followed Francillon-Vieillot et al. (1990). We used the term “structural fibers” to refer to the mineralized collagen fibers fully incorporated in the mineralized bone matrix (Scheyer and Sander 2004). We adopted the term “interwoven structural fiber bundles” (ISFB; sensu Scheyer and Sander 2004) to describe bundles of structural fibers within the bone matrix. In the core, the

structural fibers are sparser, while in the cortex, they are more organized (e.g., the orthogonal arrangement in nodosaurids; perpendicular to the external surface in ankylosaurids; Burns and Currie 2014).

Paleohistology

The paleohistological protocols followed those commonly used in current literature (Chinsamy and Raath 1992; Chinsamy 2005; Lamm 2013). We embedded the samples into clear epoxy resin Resapol T-208 and sectioned them with a precision router. The plane of section in CAV-A4 followed the longitudinal keel, which exhibits the widest preserved bone area to section. The sectioning plane was indeterminate in the other specimens due to their fragmentary nature. The blocks were fixed in a slide and polished in a wet metallographic polishing machine, Arotex AROPOL E until they reached a final thickness of 30–60 microns. The photomicrographs were taken under a cross-polarized microscope (Zeiss) and photographed by an Axiocam.

Morphometric Dataset

Most of the ankylosaur dataset was compiled from Burns and Currie (2014). We added new measurements from the literature, comprising the nodosaurid *Ahshislepelta* (Burns and Sullivan 2011), the ankylosaurine UMNH 12675 (Loewen et al. 2013), *Antarctopelta* (Cerdeña et al. 2019) and the titanosaurs *Saltasaurus* (Chinsamy et al. 2016), and MCS-Pv 181 and MCS-Pv 182 (Cerdeña et al. 2015). We included titanosaurs due to their cortex and core microstructure being quite like the one observed in some ankylosaurians, therefore having the potential of being mistakenly identified as ankylosaurian osteoderms or vice versa. Although more titanosaur specimens have been described with osteoderms (e.g., D’Emic et al. 2009; Curry Rogers et al. 2011), we could not include them here, because (1) the photomicrograph does not figure the entire section—with cortex and core (e.g., Curry Rogers et al. 2011); (2) the published figures do not identify the boundaries of cortex and core—as in *Rapetosaurus* (see Curry Rogers et al. 2011)—and the figure is not in an adequate quality to delimit them; and (3) the

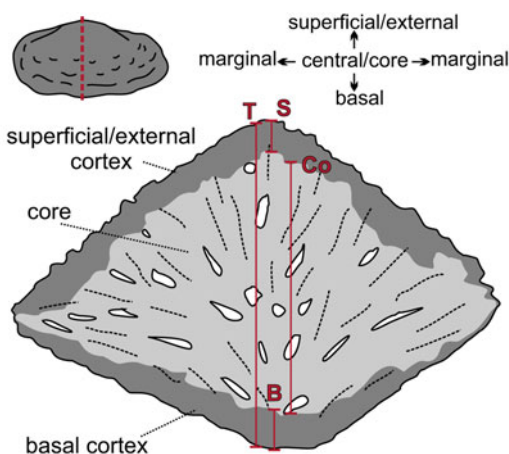


FIGURE 1. Schematic osteoderm showing the anatomical terminology adopted and the linear measurements performed here. Abbreviations: B, basal thickness; Co, core thickness; S, superficial thickness; T, total thickness.

literature data only reported the external anatomy of the osteoderms (e.g., D’Emic et al. 2009).

Our dataset is available in Brum et al. (2023) and comprises 8 ankylosaurid, 16 nodosaurid, 3 titanosaurian, 2 indeterminate ankylosaurian, and 2 *Antarctopelta* (of controversial taxonomy and systematic affinities) osteoderms, besides 2 of the new specimens reported here—we could not measure CAV-A10, as it is too fragmentary. The images obtained from the literature were measured using ImageJ 1.52a (Schneider et al. 2012).

Linear measurements of the osteoderms were converted into relative osteoderm ratio thickness (Fig. 1), following Burns and Currie (2014), for a direct shape comparison (i.e., excluding size as a variable): superficial index—superficial cortex/total osteoderm ($SI = 100 \cdot S/T$); basal index—basal cortex/total osteoderm ($BI = 100 \cdot B/T$); cortical index ($CI = 100 \cdot (S + B)/T$); and core index—core/total osteoderm ($CoI = 100 \cdot Co/T$). All values were log-transformed (\log_{10}) for subsequent statistical analyses.

Statistical Analyses

We performed ordinary least-square (OLS) linear regressions to evaluate the correlation between morphometric variables and to find a predictor model for dinosaurian osteoderm shape. Although some studies suggest the utilization of reduced major axis (RMA) linear regressions instead of OLS for inferring species allometric relationships (e.g., Warton et al. 2006), we followed the recommendation of Kilmer and Rodríguez (2017) on using OLS instead of RMA. The RMA uses the ratio of the standard deviation between the y- and x-axes to calculate the slope, as it assumes that the error distribution should be proportional between the two axes (i.e., assumes symmetry in the error distribution between axes). However, this is rare in allometric relationships, as the x-axis in these almost always refers to body size (constant variable), while the y-axis refers to various trait values. On the other hand, OLS considers the covariation between axes relative to the variation on the x-axis to calculate the slope (not assuming symmetry in error distribution between axes). This reduces error when estimating the angular

coefficient, achieving functional scaling relationships (Kilmer and Rodríguez 2017). Our study focuses on the trait–trait relationship (e.g., $SI \times CI$), with most of our variables being interchangeable between axes. However, we cannot assume a symmetric distribution of error among variables, because measurements for each variable were taken by different authors, and so error distribution is likely to be asymmetric between variables (and thus between axes). Therefore, we chose to employ OLS instead of RMA.

To test whether each osteoderm ratio variable can discriminate between different groups of dinosaurs (ankylosaurids, nodosaurids, and titanosaurs) for taxonomic purposes, we performed nonparametric Kruskal-Wallis (KW) tests. Our choice for nonparametric tests is due to the small sample size for each group and the nonnormal distribution of the data (see the tests for normality in Supplementary Fig. 2). Group assignment was based on the results of the phylogenetic analysis conducted here (see “Ankylosaur Phylogeny and Assignment of CAV Specimens”). The indeterminate ankylosaurians (TMP 1998.98.1 A.2 and TMP 1987.113.4 A.1) and the osteoderms of *Antarctopelta* were not included within any of the three dinosaurian groups due to (1) the uncertain phylogenetic placement of *Antarctopelta* between previous and more recent phylogenetic analyses (e.g., Arbour and Currie 2016; Arbour et al. 2016; Soto-Acuña et al. 2021; Frauenfelder et al. 2022); and (2) recent analyses inferring *Antarctopelta* as external to the two main ankylosaurid groups, being the only early-diverging ankylosaurian included here (Soto-Acuña et al. 2021; Frauenfelder et al. 2022; herein).

Further, we compared the decline in relative overall cortical thickness in osteoderms among groups using an exponential bivariate regression (EBR) between CI and T, as previously performed by Burns and Currie (2014). In the latter, specimens were assigned to three ankylosaurian groups—Ankylosauridae, Nodosauridae, and “Polacanthidae” (Burns and Currie 2014: fig. 8). Most of our group assignments correspond to theirs (see Supplementary Table 1), except “Polacanthidae,” which are assigned to nodosaurids herein based on their

more recent phylogenetic classification (e.g., Soto-Acuña et al. 2021; this study, see “Ankylosaur Phylogeny and Assignment of CAV Specimens”). Our new dataset is further distinct from Burns and Currie (2014), as it includes the ankylosaurid UMNH 12675, the nodosaurids *Ahshislepelta*, and the ankylosaur *Antarctopelta* (see Supplementary Table 1). To test which group best fit the EBR, we used the Akaike information criterion (AIC).

To assess the morphospace occupation and test group discrimination, we performed multivariate linear discriminant analyses (LDA). Although the principal component analysis (PCA) partially overlaps the observed data distribution depicted by OLS, we report it to provide an additional and easier visualization of morphospace occupation of ankylosaurian groups. All statistical analyses were performed in the software PAST v. 4.02 (Hammer et al. 2001), with $\alpha = 0.05$.

Phylogenetic Analysis

We scored the CAV specimens in the data matrix of Soto-Acuña et al. (2021), which resulted in 68 taxa and 189 characters (all treated as unordered, thus treating all possible state transitions as equally likely). The dataset includes 23 characters related to postcranial osteoderms and 4 related to osteoderm microstructure (characters 157 to 160). The entire data matrix is available in Brum et al. (2023).

We performed equal weights maximum parsimony analyses in TNT v. 1.5 (Goloboff and Catalano 2016) using traditional search (tree bisection reconnection), with 1 random seed, 6000 replicates, and 100 trees to save per replication. We retained suboptimal trees by 10 steps with a 0.01 relative difference. The first analysis was conducted without the new CAV specimens to track the microstructural osteoderm characters. The second analysis included the CAV specimens to verify that we could assign them to an ankylosaur ingroup solely by osteoderm microstructural characters.

Institutional Abbreviations

Centro Acadêmico de Vitória, Universidade Federal de Pernambuco, Pernambuco, Brazil (CAV-A); Colección Paleontológica de Coahuila, Museo del Desierto, Saltito, Mexico (CPC);

Delaware Museum of Natural History, Delaware, U.S.A. (DMNH); Goldfuss-Museum, Steinmann Institute for Geology, Mineralogy and Paleontology, University of Bonn, Germany (IPB); Museo Regional Cinco Saltos, Río Negro Province, Argentina (MCS-Pv); Museo Municipal Carmen Funes, Plaza Huincul, Neuquén, Argentina (MLP); Museum of Western Colorado, Grand Junction, Colorado, U.S.A. (MWC); Natural History Museum, London, U.K. (NHMUK); Instituto Miguel Lillo, Tucumán, San Miguel Tucumán, Argentina (PVL); State Museum of Pennsylvania, Harrisburg, Pennsylvania, U.S.A. (SMP); Royal Tyrrell Museum of Palaeontology, Drumheller, Alberta, Canada (TMP); University of Alberta Laboratory for Vertebrate Paleontology, Edmonton, Alberta, Canada (UALVP); Utah Museum of Natural History, University of Utah, Utah, U.S.A. (UMNH); Zoological Institute of Paleobiology, Polish Academy of Sciences, Warsaw, Poland (ZPAL).

Results

Systematics

Dinosauria Owen, 1842

Ornithischia Seeley, 1888

Thyreophora Nopsca, 1915

Ankylosauria Osborn, 1923

Nodosauridae indet. Marsh, 1890

See Figures 2–4 and Table 1.

Locality and Horizon.—The James Ross Basin outcrops are mostly represented by sequences of marine siliciclastic and volcanoclastic rocks (Barremian–Eocene; Olivero 2012b; Burton-Johnson and Riley 2015; Piovesan et al. 2021). The new specimens came from Santa Marta Cove (northeast of James Ross Island), which is marked by exposures of the upper levels of the Snow Hill Island Formation (for age and paleoenvironmental discussions, see Piovesan et al. 2021) and corresponds to the upper levels of the MG sequence (late Campanian; Olivero and Medina 2000; Olivero 2012a,b). These are the same region and levels in which *Antarctopelta* had been originally found (Salgado and Gasparini 2006; Cerda et al. 2019).

Specimen Description.—The new specimens are fragmentary and isolated unmodified osteoderms. The superficial surface of CAV-

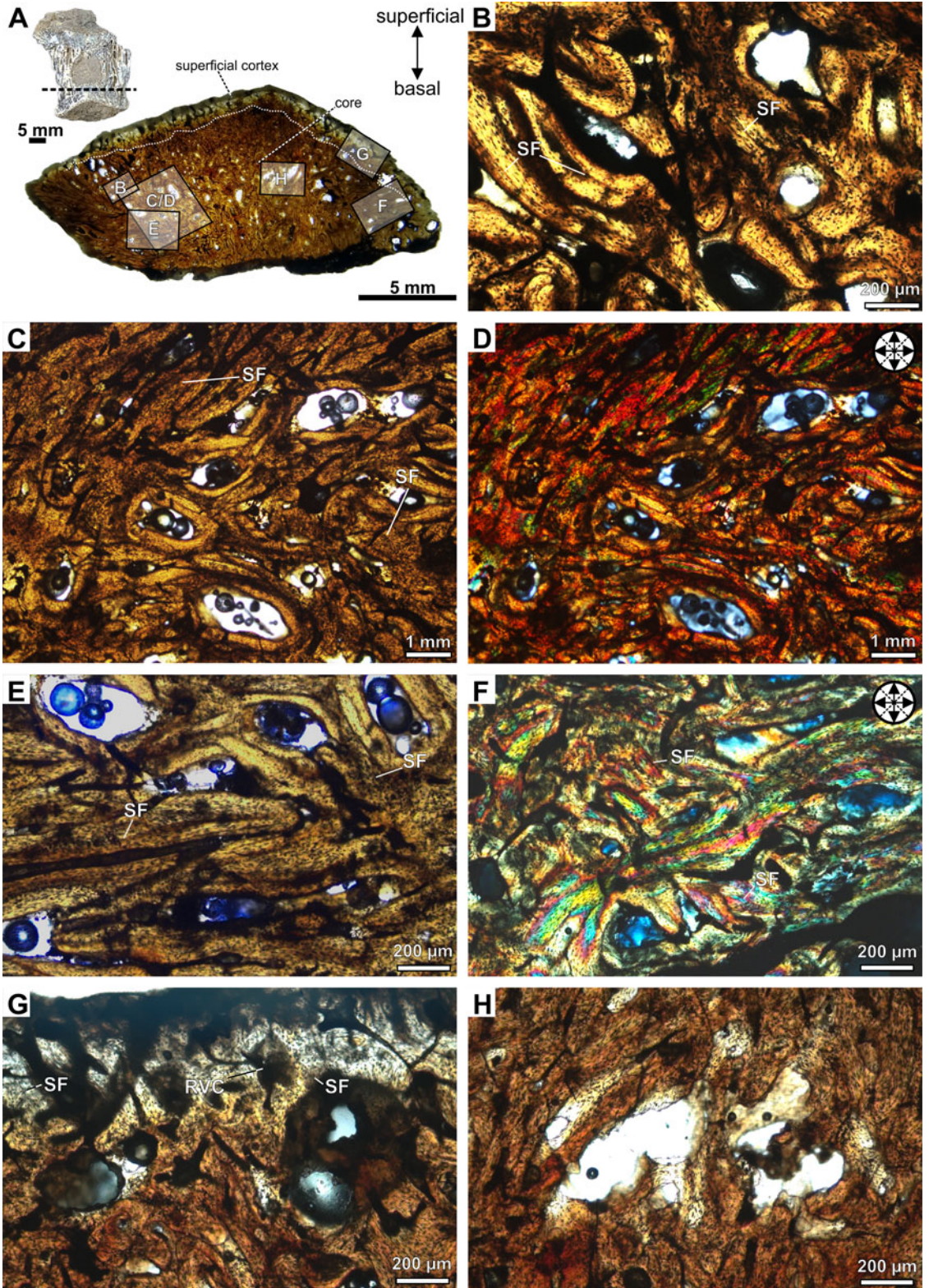


FIGURE 2. Photomicrographs of the transversal section slide of the osteoderm CAV-A4. A, Detail of the specimen and the panoramic slide. B, Detail of the alignment of osteocyte lacunae and the bone matrix organized into bundles with structural fibers, forming diffuse interwoven structural fiber bundles (ISFBs). Structural fibers assuming an orthogonal arrangement in the core under normal transmitted (C) and cross-polarized light (D). E, Detail of the ISFBs in the core region close to the basal cortex. F, Orthogonal arrangement of the structural fibers in the core, close to the margin of the osteoderm, under cross-polarized light. G, Superficial cortex in detail, with structural fibers being more perpendicular to the external surface. H, Erosion cavity with irregular surfaces, indicating an active resorption process in the core of the osteoderm. Abbreviations: RVC, reticular vascular canals; SF, structural fibers.

A4 is abraded, partially exposing the core region. Specimen CAV-A5 is rounded and exhibits a longitudinal keel on the surface. Both cross sections are triangular (Figs. 2, 3). CAV-A10 has an abraded basal region (Fig. 4), and all specimens exhibit a similar microstructure, with the core filled by a compact bone interstitial to resorption cavities. These cavities are wide and accumulate close to the basal cortex. The transition from cortical bone to the core is gradual, characterized by resorption cavities within the cortex. The osteoderms also lack densely abundant secondary (Haversian) bone, with sparse and isolated secondary osteons in the core. Few resorption cavities and rich ISFBs fill the core, which is rich in compact bone (Figs. 2–4). The ISFBs in the core are more scattered (Figs. 2B–D, and 3B), whereas they are more organized close to the external/basal and marginal surfaces of the cortex (Figs. 2E–G, and 3C–G). Specimen CAV-A10 exhibits wider erosional cavities than those observed in the other CAVs (Fig. 4A). Cross-polarized light reveals that the fibers in both core and cortex are highly orthogonally organized (Figs. 2C–F, 3B–F, and 4D–F). The bone matrix is rich in flattened osteocyte lacunae, which are aligned with the main directions of the ISFBs (Fig. 4C–F). Additionally, osteocyte lacunae lack preserved canaliculi. The vascular canals are mostly reticular (Figs. 2G, and 3B–G), but in the core of CAV-A10, they are mostly longitudinal (Fig. 4E,F).

The cortical bone is compact and poorly vascularized. The cortical bone of the core is thicker than the superficial cortical bone (Table 1). Further, some erosional cavities exhibit irregular inner margins, indicating an active resorption process (Figs. 2H, and 3H). The basal cortex is mostly absent in both CAV-A5 and CAV-A4. In cross section, the basal region is slightly abraded and does not show the decrease in resorption cavities

observed in the superficial cortex. The structural fibers are more numerous and more organized in the basal region (Fig. 3C,D). Despite the core potentially being reduced in thickness due to weathering of the osteoderms, the alignment of the structural fibers in the basal region indicates that it was close to the margin—such well-organized structural fibers are characteristic of regions close to the cortex. If not absent, the basal cortex was at least relatively very thin compared with other ankylosaurian osteoderms.

Bone Origin, Growth, and Ontogeny

The microstructure of the CAV specimens resembles metaplastic bone features in osteoderms, as pointed out by Main et al. (2005: p. 303), characterized by “poorly vascularized, amorphous dermal bone tissue in which fibers are very numerous and oriented in many directions.” Another feature is the lack of canaliculi in the osteocyte lacunae (Levrat-Calviac and Zylberberg 1986). Different from neoplastic bones, metaplastic bone lacks the development of a periosteum, being formed from dense connective tissues, such as ligaments and tendons (Haines and Mohuiddin 1968; Organ and Adams 2005) and—in the case of ankylosaurian and archosaur osteoderms—from *stratum compactum* of the dermis (Scheyer and Sander 2004; Main et al. 2005; Vickaryous and Sire 2009; Cerda and Powell 2010; Scheyer et al. 2014; Cerda et al. 2015, 2019; Bellardini and Cerda 2017; Ponce et al. 2017). Although ossicles and osteoderms are both types of metaplastic bone, CAV specimens can be diagnosed as osteoderms due to the higher degree of vascularization in comparison with that observed in ossicles, as well as the structural fiber bundles being less organized. In ossicles, structural fibers form a three-dimensional mesh with bundles perpendicular to each other in all directions (e.g., de Ricqlès et al. 2001; Cerda and Powell 2010; Cerda et al. 2019).

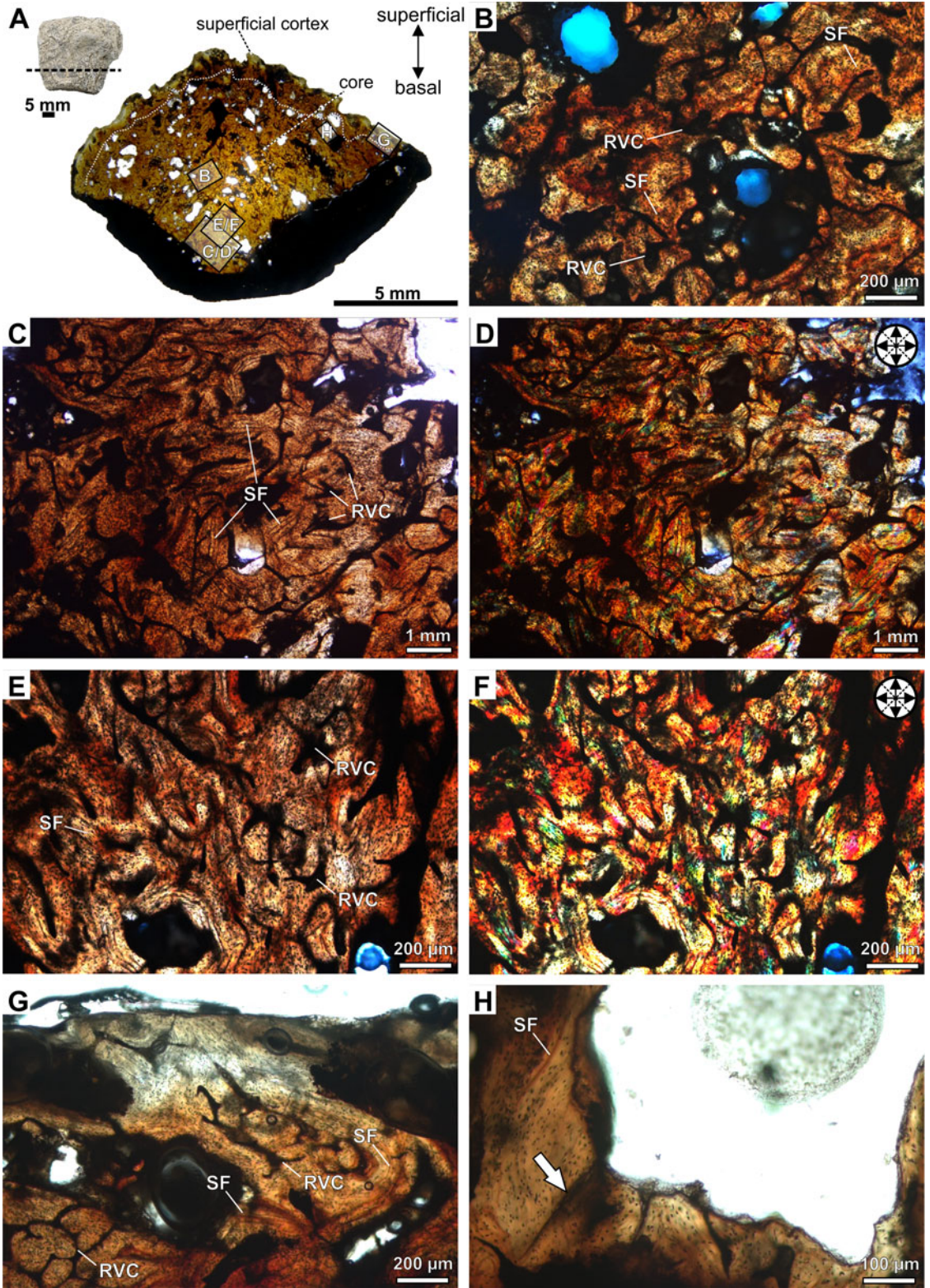


FIGURE 3. Photomicrographs of the transversal section slide of the keeled osteoderm CAV-A5. A, Detail of the specimen and panoramic slide. B, The interwoven structural fiber bundles (ISFBs) are more disorganized in the central region of the core. Orthogonal arrangement of the structural fibers in the basal region of the core, rich in reticular vascular canals, under normal transmitted (C, E) and cross-polarized light (D, F). G, Detail of the superficial cortex, with structural fibers more perpendicular to the external surface. H, The erosional cavity in the core of the osteoderm, with detail on its irregular inner margins and close to a micro-crack (arrow). Abbreviations: RVC, reticular vascular canals; SF, structural fibers.

The CAV specimens lack growth marks and dense secondary osteons (only CAV-A10 shows some isolated secondary osteons). Some ankylosaurian osteoderms are devoid of such features (Hayashi et al. 2010), whereas others have been previously described as having primary lamellar bone tissue with lines of arrested growth (LAGs) and extensive secondary reconstruction (Scheyer and Sander 2004; Main et al. 2005). Such a difference was regarded as representing distinct ontogenetic stages, with juvenile/subadult stages being characterized by the rapid growth of the bone—woven or ISFB—and further substituted in the adult stage by lamellar bone with LAGs and secondary bone through erosion/reconstruction processes (Main et al. 2005; Hayashi et al. 2009, 2010). Considering the histological ontogenetic stages proposed for *Stegosaurus* (see Hayashi et al. 2009), CAV-A4 and CAV-A5 are assigned to stage 1, characterizing juvenile/subadult individuals. CAV-A10 exhibits some secondary osteons and longitudinal vascular canals, which makes it assignable to stage 2, a subadult individual. In *Antarctopelta*—an adult close to fully grown (Cerda et al. 2019)—the erosion/reconstruction process is advanced, with some LAGs. This is markedly different from the tissues observed among CAVs. On the other hand, armadillos and crocodylians show an asynchronous development of the osteoderms along the anteroposterior regions of the body (Vickaryous and Hall 2006, 2008), and a similar pattern has already been observed in dinosaurs among juveniles of *Pinacosaurus* (Burns et al. 2011; Burns and Currie 2014). Therefore, this ontogenetic inference is only tentative, and we urge caution in inferring an ontogenetic stage to the whole organism based solely on isolated osteoderms, due to the different timing in osteoderm development in relation to the whole organism (Main et al. 2005; Hayashi et al. 2009, 2010) and the lack of detailed studies in the variation

along the anteroposterior axis of ankylosaurians.

Microstructural Comparisons

Osteoderms rich in ISFBs are common to dinosaurs (titanosaurs and thyreophorans; Salgado 2003; Scheyer and Sander 2004; Cerda and Powell 2010; Hayashi et al. 2010; Burns and Currie 2014; Chinsamy et al. 2016). The core of the CAV specimens is filled with a few cavities, as similarly observed in other ankylosaurians (Burns and Currie 2014) and in the titanosaur MCS-Pv 181 and MCS-Pv 182 (Cerda et al. 2015). However, the bone matrix of all CAVs is organized in bundles with an alignment of the osteocyte lacunae. Such a feature more closely resembles the pattern found in ankylosaurians (see Burns and Currie 2014) than in titanosaur, which do not show a clear bundle pattern (osteocyte lacunae are less organized) and are richer in woven bone (see Cerda and Powell 2010; Cerda et al. 2015; Chinsamy et al. 2016; Maidment et al. 2021).

The compact bone in the core is present in both late-diverging ankylosaurids and nodosaurids (Burns and Currie 2014). The few resorption cavities and secondary osteons differ from the ones observed in the early-diverging nodosaurids *Gastonia* (DMNH 49754-1) and *Gargoyleosaurus* (DMNH 27726) and in ankylosaurids, in which this region of the osteoderm is marked by large cavities and remodeled trabecular bone (Scheyer and Sander 2004; Hayashi et al. 2010; Burns and Sullivan 2011; Burns and Currie 2014). Osteoderm thickness is like that of nodosaurids (Hayashi et al. 2010; Burns and Currie 2014), just like the orthogonal arrangement of the ISFBs (Scheyer and Sander 2004; Burns and Currie 2014). The thin (or absent) basal cortex is regarded as synapomorphic to nodosaurids (Scheyer and Sander 2004; Burns and Currie 2014).

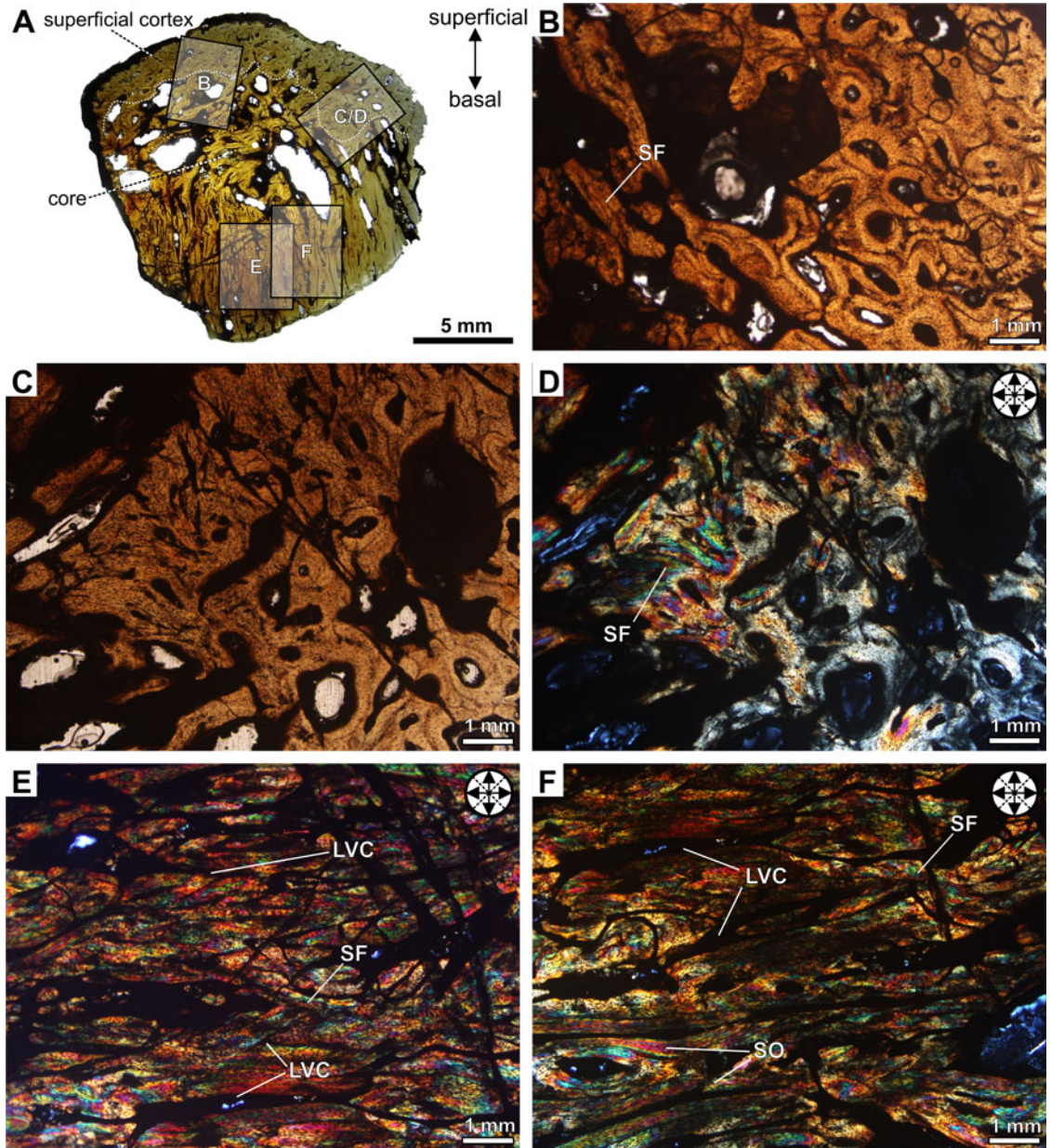


FIGURE 4. Photomicrographs of the osteoderm CAV-A10. A, Detail of the specimen and panoramic slide. B, Photomicrograph of the external cortex rich in vascular canals with ISFBs. Detail of the orthogonal arrangement of the interwoven structural fiber bundles (ISFBs) in the contact between the core and external cortex under normal transmitted (C) and cross-polarized light (D). E, F, A core region rich in longitudinal vascular canals and showing an orthogonal arrangement of ISFBs under cross-polarized light. Abbreviations: LVC, longitudinal vascular canals; SF, structural fibers; SO, secondary osteons.

Among nodosaurids, the shape of the cross section in all CAVs differs from that observed in the thoracic osteoderm of *Edmontonia* (TMP 1998.98.1) and from osteoderms of *Glyptodonta* (SMP VP-1580; Burns and Currie 2014),

in which the superficial and basal cortices are aligned. However, the microstructure of CAVs is like that of *Edmontonia* and *Glyptodonta*, in that there are ISFBs, no clear stratification between the cortex and core, and few scattered

TABLE 1. Thickness measurements of the specimens from James Ross Island. The values in W, S, B, S+B, and Co are in millimeters. Abbreviations: B, basal cortical bone thickness; BI, basal index; CI, cortical index; Co, core thickness; CoI, core index; S, surface cortex thickness; SI, superficial index; T, total osteoderm thickness; W, maximum width of whole osteoderm. *Partial measurement.

| Specimens | W | S | B | S+B | Co | T | SI | BI | CoI | CI |
|-----------|-------|-------|---|-------|-------|--------|--------|----|--------|--------|
| CAV-A4 | 32.23 | 0.481 | — | 0.481 | 8.756 | 9.348 | 5.145 | — | 93.667 | 5.145 |
| CAV-A5 | 33.61 | 0.874 | — | 0.874 | 7.805 | 8.693 | 10.054 | — | 89.785 | 10.054 |
| CAV-A10 | — | 2.459 | — | — | — | 16.87* | — | — | — | — |

secondary osteons. The CAV specimens differ from *Sauropelta* (DMNH 18206; Burns and Currie 2014) in the stratification between core and cortex, marked by secondary osteons. Although the shape of the CAVs is quite like the dermal plate of *Antarctopelta* (Cerda et al. 2019), it differs from the latter by the presence of trabeculae composed of secondary lamellar bone in *Antarctopelta*.

Dinosaurian Osteoderm Thickness Patterns and Linear Model

The OLS indicates a strong positive isometric relationship between Co and T among dinosaurian osteoderms (Fig. 5A)—see “Morphometric Dataset” for morphometric variable abbreviations. Among the relative thickness indices, the SI exhibits a positive isometric relationship with CI and a positive allometry relationship with CoI. The strongest correlation was observed between Co and T ($R^2 = 0.962$, $p = 4.235 \times 10^{-19}$; Fig. 5A), of which its linear function is:

$$\log \text{Co} = 1.169 \log T - 0.304 \quad (1)$$

This function provides a model to estimate the mean of the core thickness or the mean of the total thickness in cases in which the cortical bones are only partially preserved.

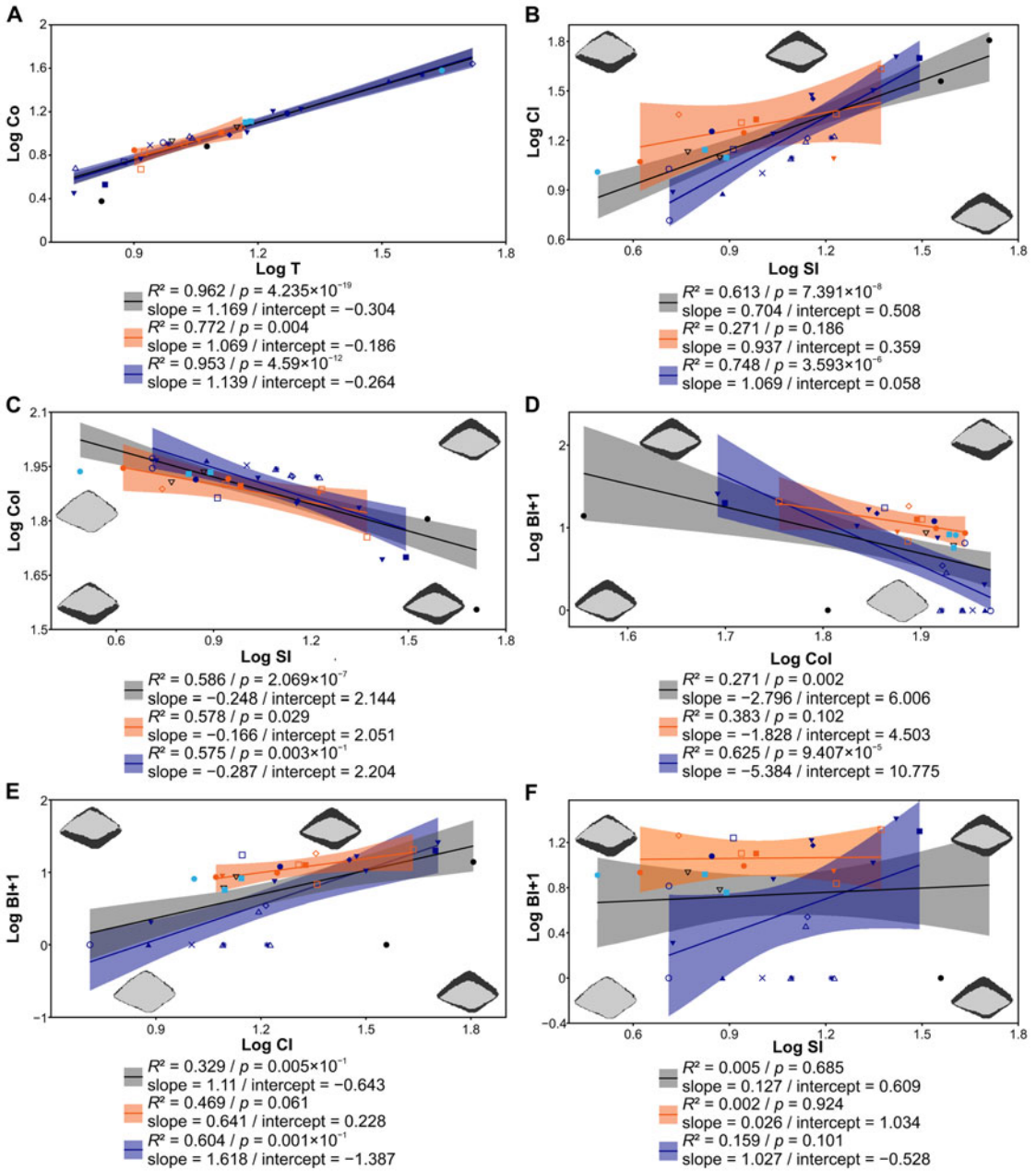
Osteoderm Thickness Variations between Groups

We detect a linear correlation between CI and SI when considering all specimens in general and in the subsample, including nodosaurids only ($R^2 = 0.613$, $p = 7.391 \times 10^{-8}$; and $R^2 = 0.748$, $p = 3.593 \times 10^{-6}$, respectively; Fig. 5B), but not when considering Ankylosauridae only ($R^2 = 0.271$, $p = 0.186$). The CoI and SI are slightly correlated between all groups ($R^2 = 0.586$, $p = 2.069 \times 10^{-7}$ for all specimens;

$R^2 = 0.578$, $p = 0.029$ for ankylosaurids; and $R^2 = 0.575$, $p = 0.003 \times 10^{-1}$ for nodosaurids; Fig. 5C). However, there is no clear correlation between BI and the other parameters (considering all specimens: $R^2 = 0.271$, $p = 0.002$ for CoI; $R^2 = 0.329$, $p = 0.005 \times 10^{-1}$ for CI; and $R^2 = 0.005$, $p = 0.685$ for SI; Fig. 5D–F). The only exceptions are BI \times CoI and BI \times CI in nodosaurids ($R^2 = 0.625$, $p = 9.407 \times 10^{-5}$; and $R^2 = 0.604$, $p = 0.001 \times 10^{-1}$, respectively; Fig. 5D,E). Therefore, the most informative parameters of covariation among titanosaurs and ankylosaurians comprise SI, CI, and CoI. The OLS indicates a slight shift between ankylosaurids and nodosaurids when contrasting SI with both CI and CoI—especially SI and CI, despite the lack of correlation between these two parameters among ankylosaurid osteoderms ($R^2 = 0.271$, $p = 0.186$; Fig. 5B).

The univariate KW analysis indicates no clear difference between medians among taxonomic groups under any of the four parameters tested here (Table 2). The box plot indicates a slight difference between ankylosaurids and nodosaurids under BI and CoI, but there is a large overlap in the range between these groups (Fig. 6). Therefore, osteoderm morphometric data are of very limited value to distinguish between ankylosaurian groups given the most recent systematic classification of this group (Soto-Acuña et al. 2021; see “Ankylosaur Phylogeny and Assignment of CAV Specimens”).

The relative thickness of the cortex (CI) decreases exponentially in comparison to the total thickness (T) of the osteoderm among ankylosaurians, being the thinnest among nodosaurids (Fig. 7), as initially suggested by Burns and Currie (2014). Considering T as a proxy for osteoderm size, such a relationship suggests an allometric decrease. Our comparisons between our EBR and that observed in Burns and Currie (2014) show higher AIC



Ankylosauridae

- Ankylosauridae indet. (TMP 1985)
- *Euoplocephalus tutus*
- Ankylosauridae indet. (ZPAL)
- ◇ *Pinacosaurus grangeri*
- * Ankylosaurinae indet.

Titanosauria

- *Saltasaurus loricatus*
- Titanosauria indet.

Nodosauridae

- ◇ *Edmontonia* sp.
- *Sauropelta edwardsorum*
- ▲ *Glyptodontopelta mimus*
- * Nodosauridae indet. (TMP)
- CAV-A4
- × CAV-A5

- *Ahshislepelta minor*
- *Gargoyleosaurus parkpini*
- ▼ *Gastonia* sp.
- *Mymoorapelta mayisi*
- *Polacanthus foxii*

- Ankylosauria indet. (TMP)
- ▽ *Antarctopelta oliveroi*

Silhouette of osteoderm in cross-section

- Grey: General linear model
- Orange: Ankylosauridae linear model
- Blue: Nodosauridae linear model

FIGURE 5. Ordinary least squares (OLS) based on core osteoderm (Co), total thickness of osteoderm (T), cortical index (CI), core index (CoI), superficial index (SI), and basal index (BI) among dinosaurian osteoderms. A, The correlation between Co and T is strong in general and between all groups. B, Although osteoderms, in general, have a clear correlation between CI and SI, only nodosaurids have a clear correlation in comparison to ankylosaurids. C, All the osteoderm groups have a moderate correlation between CoI and SI. Only the osteoderms of nodosaurids have a moderate correlation with BI and CoI (D) and BI and CI (E). F, The relationship between BI and SI has no clear correlation. The silhouette of the osteoderm cross section in the graphs indicates the osteoderm shape deformation along the main axes.

indices than in the latter. Ankylosaurids were the group that best fits the EBR model (AIC = 653.71; Fig. 7B). The inclusion of “polacanthids” into nodosaurids could contribute to the increase of AIC compared with the models in Burns and Currie (2014).

The lowest CI is observed among most nodosaurids and titanosaurs (Fig. 7), with CAV-A4 exhibiting the lowest CI and T compared with all other osteoderms analyzed. The nodosaurids *Edmontonia*, *Sauropelta*, TMP 1967.10.29, and the titanosaur *Saltasaurus* exhibit the highest T values, although their CI values are nearly the same as most other nodosaurids. The CI overlaps between all ankylosaurian groups and indicates that the assessment of ankylosaurids as “thin-walled” osteoderms is subjective (Burns 2008; Burns and Currie 2014). The expression “thin-walled” is also vague and could also refer to low CI values rather than T, but our assessments do not indicate low CI for ankylosaurids. Instead, we find that low CI is common among nodosaurids and ankylosaurids, with later-diverging nodosaurids having an even lower CI than ankylosaurids.

Morphospace Occupation of Dinosaurian Osteoderms

We performed the PCA and LDA with the indices that have a significant linear relationship—CI, CoI, and SI (Fig. 8, Supplementary Fig. 3). SI exhibits a positive linear relationship with CI and a weak negative linear relationship with CoI (Figs. 5B,C, and 8). SI is

the main predictor of group membership (LD 1; Supplementary Fig. 3); although the LDA indicates that it could not strongly discriminate between groups (58.62% of certainty). The OLS and PCA reveal that most of the data variation is explained by changes in relative cortical thickness (CI) mostly on the superficial cortex (SI) (Fig. 5; see also PC 1 in Fig. 8). Relative

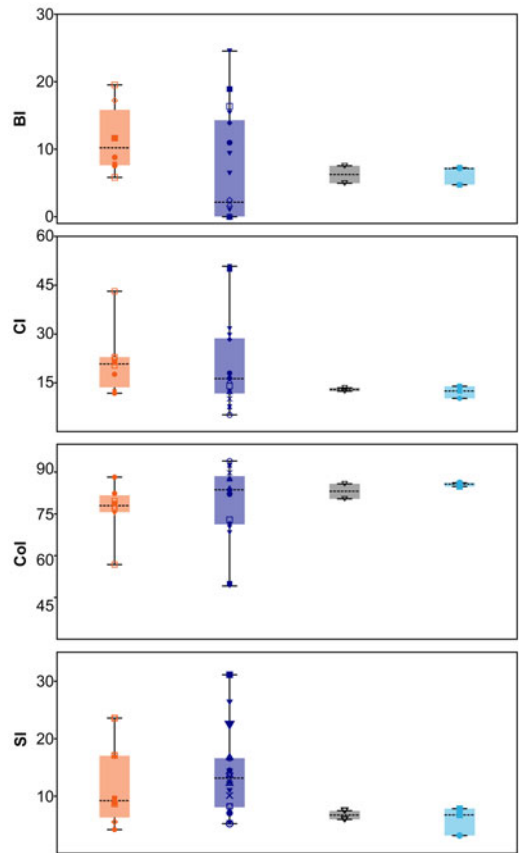


FIGURE 6. Box plots of dinosaurian osteoderm shape based on basal index (BI), cortical index (CI), core index (CoI), and superficial index (SI) ratios. The dinosaurian groups comprise ankylosaurids, nodosaurids (including the new CAV specimens), titanosaurs, and the parankylosaurian *Antarctopelta*. There is no significant difference between group medians; see Table 2 for statistical tests. The colors and symbols are the same as in the legend in Fig. 5.

TABLE 2. Univariate Kruskal-Wallis test considering ankylosaurids, nodosaurids, and titanosaurs. No value was significant ($p < 0.05$). Abbreviations: BI, basal index; CI, cortical index; CoI, core index; SI, superficial index.

| | BI | CI | CoI | SI |
|----------------|-------|-------|-------|-------|
| H [chi-square] | 9.354 | 12.19 | 11.75 | 14 |
| p | 0.22 | 0.944 | 0.109 | 0.051 |

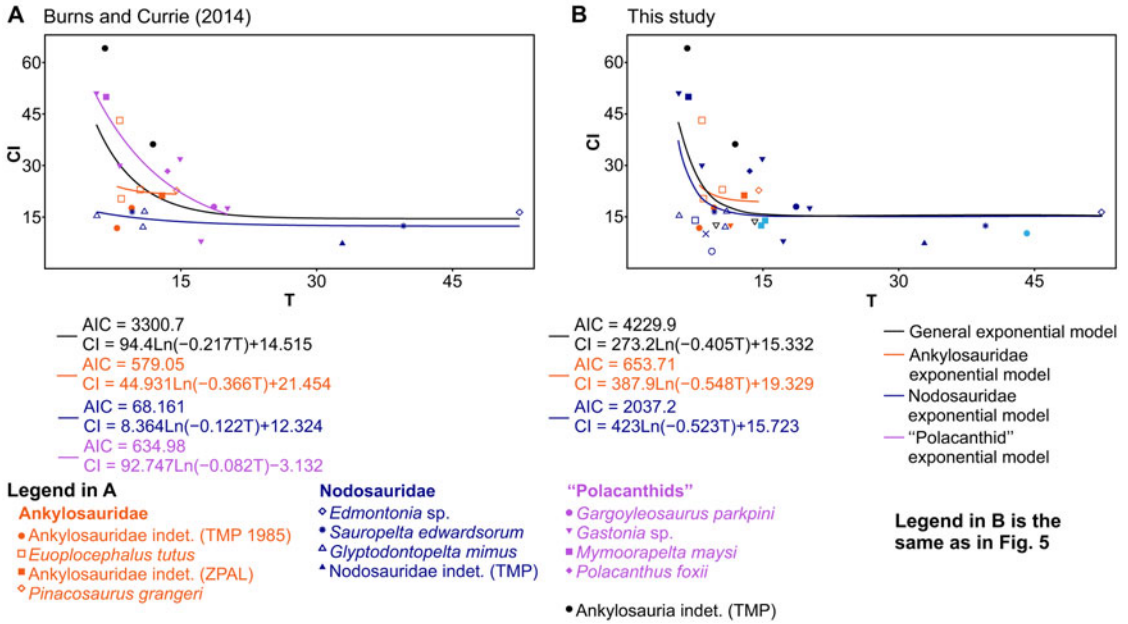


FIGURE 7. Exponential bivariate regression (EBR) between cortical index (CI) and total osteoderm (T), comparing the results of Burns and Currie (2014: fig. 8) (A) with our results (B). In both analyses, nodosaurids exhibit the lowest Akaike information criterion (AIC), indicating the best fit to the EBR. High CI marks early-diverging ankylosaurians, whereas lower CI marks nodosaurids and titanosaurs. Note that nodosaurids and titanosaurs exhibit higher T and lower CI. Names in bold were originally analyzed by Burns and Currie (2014) and in this study. The colors and symbols in B are the same as in the legend in Fig. 5.

core thickness (CoI) is the main factor responsible for the overlap between ankylosaurids, nodosaurids, and titanosaurs.

The morphospace of ankylosaurids considerably overlaps with the morphospace of

nodosaurids (Fig. 8). However, nodosaurids have a larger variance of osteoderm shape along the main axes of variation (PC 1), which reflects the enormous observed variation in cortical thickness in this group (e.g., CoI) and accounts for the vast majority of the total variation in the data (88.7%). The somewhat broader morphospace of ankylosaurids along PC 2 is mostly explained by the great degree of variation in CI and SI introduced by *Euoplocephalus* and *Pinacosaurus* (Fig. 8, Supplementary Fig. 3). Additionally, two of the indeterminate ankylosaurid specimens (TMP 1987.113.4A.1 and TMP 1998.98.1A.2) are outliers, located in a much more distant region of the morphospace relative to all other osteoderms that could be confidently identified to the family level.

Notably, the larger morphospace occupation of nodosaurids along the first major axis (PC 1) is highly influenced by the inclusion of the new materials described here from Antarctica (most notably, CAV-4). The latter has expanded the nodosaurid morphospace into a region previously unoccupied by any other group of

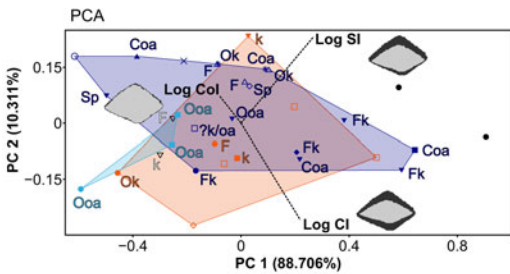


FIGURE 8. Result of the PCA. The silhouette of the osteoderm cross section within graphs indicates the osteoderm shape deformation along the main axes. Both superficial index (SI) and cortical index (CI) contribute to most of the variation in the morphospace observed among ankylosaurian osteoderms. Abbreviations: Coa, circular off-apex osteoderm; F, flat osteoderm; Fk, flat keeled osteoderm; k, keeled osteoderm, but unknown shape; oa, off-apex osteoderm, but unknown shape; Ooa, oval off-apex osteoderm; Ok, oval keeled osteoderm; Sp, spine. The colors and symbols are the same as in the legend for Fig. 5.

dinosaurs. This suggests a unique osteoderm morphology for the new Antarctic specimens compared with other nodosaurids, ankylosaurians, and dinosaurs. The large variation in CoI among nodosaurids is responsible for the unique area of the morphospace occupied by this group, including the new CAV specimens. This suggests a reduction in cortical thickness on the osteoderms of some nodosaurids compared with other ankylosaurians, which have retained much thicker cortical bone.

Titanosaurs occupy a much smaller morphospace than all three groups of ankylosaurians, also partially overlapping with nodosaurids. However, we note that we have few data points (only three) for titanosaurs; the morphospace occupation by the group could be much broader.

Ankylosaur Phylogeny and Assignment of CAV Specimens

Both phylogenetic and paleohistological data indicate a division of ankylosaurians into two main groups: Ankylosauridae and Nodosauridae (Hill et al. 2003; Scheyer and Sander 2004; Hayashi et al. 2010; Burns and Currie 2014; Arbour and Currie 2016; Arbour et al. 2016; Brown et al. 2017; Rivera-Sylva et al. 2018; Fig. 9A,B). The group “Polacanthidae” (or “Polacanthinae”) was recovered as paraphyletic here, as in previous phylogenies (Hill et al. 2003; Arbour and Currie 2016; Arbour et al. 2016; Brown et al. 2017; Rivera-Sylva et al. 2018; Soto-Acuña et al. 2021; Frauenfelder et al. 2022). Most “polacanthids” are inferred as early-diverging nodosaurids (e.g., *Polacanthus*, *Gastonia*, and *Mymooropelta*; Fig. 9). Regarding microstructural differences, ankylosaurids have been described as possessing thin-walled osteoderms, with extensive Haversian bone and perpendicular organized structural fibers; nodosaurids exhibit thin/absent basal cortex and highly ordered orthogonal structural fibers; while “polacanthids” have a similar thickness with ankylosaurid osteoderms, but the structural fibers are more diffuse (Scheyer and Sander 2004; Burns and Currie 2014). Our results indicate that these osteoderm features are widespread among ankylosaurians, and only the presence of Haversian bone and lamellar bone in the superficial cortex distinguish nodosaurids from other ankylosaurians. Despite the presence

of few osteoderm phylogenetic characters and taxa scored in the matrix, these were sufficient to recover the family-level placement of the new (CAV) specimens from Antarctica (Fig. 9B).

Discussion

Osteoderm Microstructure and Evolution

Nodosaurids and titanosaurs have much thinner osteoderm cortices compared with early-diverging ankylosaurids (Figs. 5–8). This could be associated with structural constraints, such as the limitation of nutrient circulation in osteoderms due to the lack of canaliculi (Haines and Mohuiddin 1968). A few titanosaur osteoderms exhibit wide vascular canals and a network of cavities in their osteoderms (Cerdeja and Powell 2010; Curry Rogers et al. 2011; Cerdeja et al. 2015), but this is not the case among the titanosaurs sampled here, whose core structure is much more like that found in ankylosaurians. Although some previous studies indicated the presence of vascular pits in ankylosaurian osteoderms, this is restricted to only a few specimens (Scheyer and Sander 2004; Hayashi et al. 2010; Burns and Currie 2014). Therefore, late-diverging nodosaurids, and the sampled titanosaurs, may have compensated for the nutritional circulatory limitations imposed by the increase in core volume (Co; Fig. 5A) and total osteoderm thickness (T) by reducing their superficial and basal cortical thickness. The convergent evolution of cortical thickness reduction in these distantly related lineages suggests that the decrease of core density is a physiological adaptation for coping with large absolute osteoderm size.

However, we caution against establishing a direct association between cortical thickness and core density. CAV materials have a thin cortex and compact cores (Figs. 2–4, 7), whereas other nodosaurid and titanosaur osteoderms have a thinner cortex and less dense core compared with the osteoderms of other ankylosaurians (e.g., *Gastonia*, *Euoplocephalus*, *Nodocephalosaurus*, and *Saichania*). Although the physiological adaptation is a strong constraint to the osteoderm size and cortical and core thicknesses, other factors could be contributing to this balance (e.g., osteoderm shape,

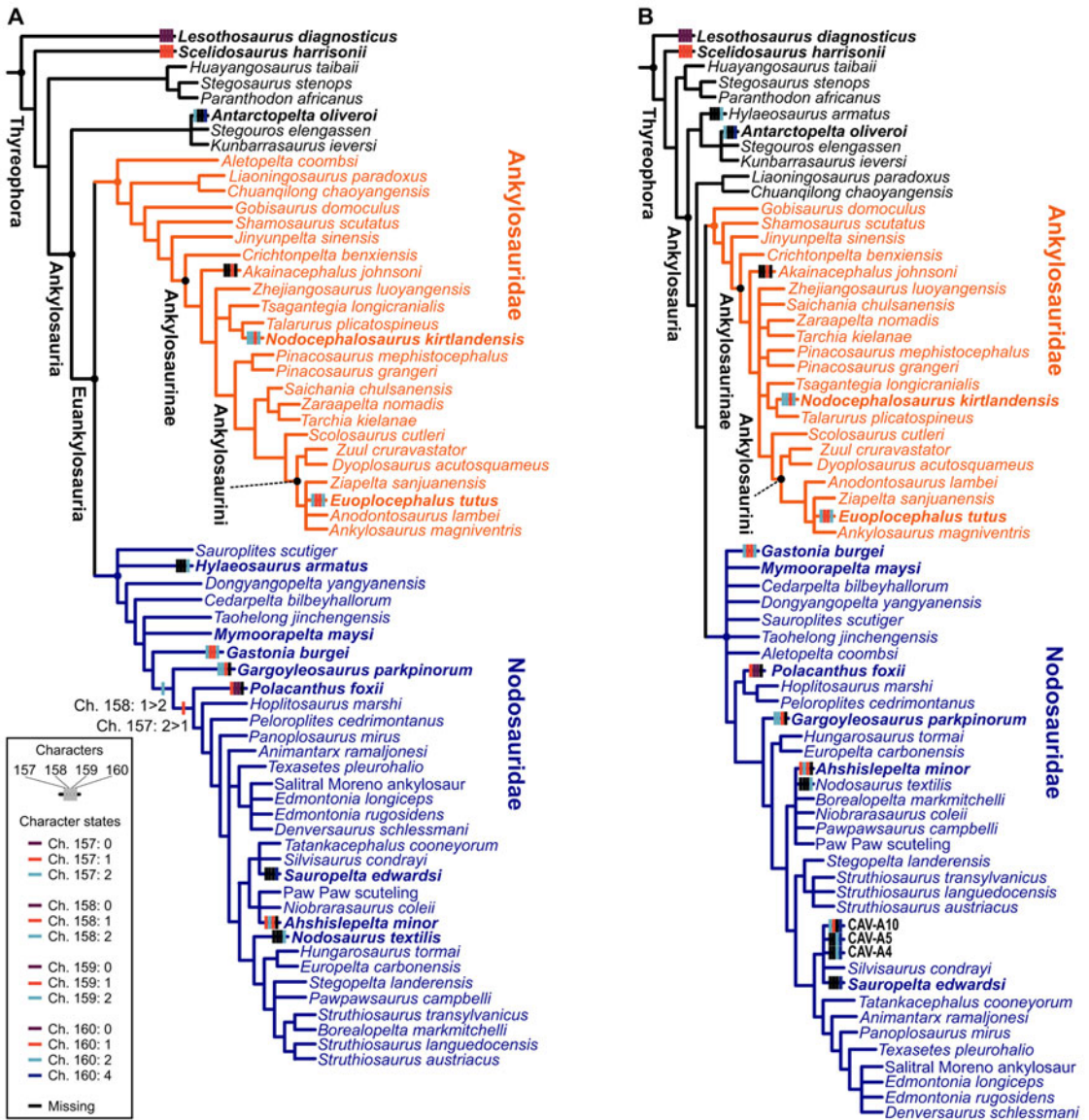


FIGURE 9. Phylogenetic results from the dataset of Soto-Acuña et al. (2021). Strict consensus of the three most parsimonious trees (MPTs) of 695 steps, without CAV specimens in (A). Strict consensus of seven MPTs of 697 steps each including CAV specimens (B). Osteoderm characters mapped on the trees: Ch. 157: external cortical histology of skeletally mature osteoderms: no osteoderms (0) lamellar bone (1), ISFB (2); Ch. 158: Haversian bone in osteoderms: no osteoderms (0) absent in core of skeletally mature osteoderms (1), maybe present in the core of skeletally mature osteoderms (2); Ch. 159: basal cortex of skeletally mature osteoderms: no osteoderms (0) present (1), absent or poorly developed (2); Ch. 160: structural fiber arrangement in osteoderms: no osteoderms (0) structural fibers absent (1), reaches orthogonal arrangement near osteoderm surfaces (2), diffuse throughout (3), highly ordered sets of orthogonally arranged fibers in the superficial cortex (4). See Brum et al. (2023) for a detailed common synapomorphy list.

biomechanics, variation in developmental timing along the body axis).

Additionally, we observe that “polacanthid” *Gastonia*, *Mymoorapelta*, *Polacanthus*, *Gargoylesaurus*, and *Ahshislepelta* (now considered

early-diverging nodosaurids; Fig. 9) mainly occupy a region of morphospace that overlaps with some ankylosaurids (Fig. 8). This partially reflects their phylogenetic instability (Thompson et al. 2012; Arbour and Currie 2016; Arbour

et al. 2016; Brown et al. 2017; Rivera-Sylva et al. 2018) and supports previous claims that there is no clear distinction between ankylosaurid and “polacanthid” osteoderms (Burns and Currie 2014). Our results suggest that the region of morphospace occupied by both early-diverging nodosaurids (“polacanthids”) and ankylosaurids—high thickness of compact bone layers, especially the superficial cortex—represents the ancestral morphospace in the early evolution of ankylosaurians. These hypotheses would be supported even in the former classification of “polacanthid” as early-diverging ankylosaurians (outside ankylosaurids and nodosaurids; Scheyer and Sander 2004; Hayashi et al. 2010; Burns and Currie 2014).

Our phylogenetic results agree with recent analyses (Soto-Acuña et al. 2021) in recovering *Antarctopelta* as closely related to *Stegouros* and *Kunbarrasaurus*, forming the new early-diverging ankylosaur group Parankylosauria, and also reveal the historically phylogenetic unstable “polacanthids” to be early-diverging nodosaurids (Soto-Acuña et al. 2021; Fig. 9A,B). However, our results indicate that the osteoderm characters of *Antarctopelta* resemble those observed in late-diverging nodosaurids and in CAV specimens (Fig. 9B).

The main difference between ankylosaurids and late-diverging nodosaurids is the basal cortex (BI; as in Burns and Currie 2014) and the thickness of the core (CoI; not the occurrence of cavities), as discussed later. The new specimens described here (CAVs) were phylogenetically inferred to be nodosaurids, and their cortex thickness indicates they have some of the thinnest cortices among nodosaurids, even if the cortex may have been partially lost due to weathering—see “Specimen Description.” We also noticed the presence of highly ordered orthogonally arranged fibers (Fig. 9B) and the wide core thickness (Fig. 8) in CAV specimens and *Antarctopelta*. This pattern and the phylogenetic analysis suggest that the CAV specimens are from late-diverging nodosaurids. Considering the recent suggestion of *Antarctopelta* as an early-diverging ankylosaurian, our results suggest a larger phylogenetic diversity of Antarctic ankylosaurians, including both early- and late-diverging forms.

The Function of Body Osteoderms

The several differences observed in relative thickness and osteoderm microstructure among various groups of dinosaurs (Figs. 5–8) have led to several hypotheses surrounding their inferred function, including body armor, display, and thermoregulation (Scheyer and Sander 2004; Cerda and Powell 2010; Hayashi et al. 2010; Curry Rogers et al. 2011; Burns and Currie 2014; Cerda et al. 2015; Brown 2017; Vidal et al. 2017). The osteoderms analyzed here exhibit different morphologies (e.g., spikes, oval keeled, circular with offset apex; Fig. 8; see also Supplementary Table 1), indicating they may come from different body regions, excluding tail clubs and ossicles. The fragmentary preservation of the osteoderms prevents us from a detailed assessment of osteoderm microstructure and function across individual body regions, but the available data still provide informative insights into the function of ankylosaurian body osteoderms in general.

The association between microstructure and morphology in osteoderms enables the interpretation of multiple adaptive functions, as observed among extant reptile groups. For instance, in extant crocodylians, Sharpey’s fibers in the cortex are perpendicular to the external margin of the osteoderm, being anchored by tendon attachment—as also inferred for stegosaurids (Scheyer and Sander 2004). The presence of these fibers in crocodylomorphs contributes to the flexibility of the whole armor and improves its strength (Sun and Chen 2013). In addition, keeled body osteoderms of crocodylomorphs are more resistant to breakage relative to non-keeled forms, whereas stress tends to concentrate near pits and ridges in ornamented osteoderms, which represent areas of crack initiation and propagation (Clarac et al. 2019). However, the porosity of the core and the 3D vascular network are factors that enhance the bending stiffness and pressure absorption, as well as representing a trade-off between resistance and the physiological balance in crocodylomorphs—all of which may change throughout their ontogeny (Sun and Chen 2013; Chen et al. 2014; Clarac et al. 2019). In cordylid lizards, porous core osteoderms are fractured under relatively

low-stress pressure and exhibit lower thermal conductivity. On the other hand, compact core osteoderms are comparatively more resistant to higher pressures and exhibit higher thermal conductivity (Broeckhoven et al. 2017). Therefore, in both extant crocodiles and cordylid lizards, osteoderms have multiple functions with distinct physiological trade-offs (see Gould and Vrba 1982; Gould 1991; Buss et al. 1998).

Ankylosaurians and titanosaurs differ from crocodylians and stegosaurids in their extensive distribution of structural fibers, which indicates that osteoderms were fully surrounded by dermis (Scheyer and Sander 2004; Cerda and Powell 2010; Cerda et al. 2015). In small osteoderms of both nodosaurids and ankylosaurids, the abundance of structural fibers indicates efficient lightweight body armors (Scheyer and Sander 2004; Hayashi et al. 2010), but their arrangement within late-diverging nodosaurids is distinct in comparison to the other ankylosaurians. The highly ordered orthogonal sets of structural fibers in late-diverging nodosaurids (Burns and Currie 2014) suggest more efficiency in pressure dissipation on the dermis due to their connectivity to ossicles and adjacent osteoderms (de Ricqlès et al. 2001; Scheyer and Sander 2004). Considering their external morphology, the osteoderms of ankylosaurians and titanosaurs are keeled and are devoid of extensive superficial ornamentation, thus suggesting high-stress resistance in these groups based on data from extant crocodiles (Clarac et al. 2019). In ankylosaurians, the morphology of small body osteoderms (e.g., rounded keeled) resembles the plesiomorphic condition found in the early-diverging thyrophan *Scutellosaurus*, which was retained (or even augmented) in ankylosaurians (Main et al. 2005). The acquisition of abundant structural fibers among small osteoderms of ankylosaurians (Scheyer and Sander 2004; Hayashi et al. 2010) further suggests the body-armoring function of these osteoderms. Accordingly, the erosional cavities with irregular margins in CAVs (Figs. 2H, and 3H) indicate an active resorption process, which could reflect a response to microstructural fractures resulting from such a defensive role (see Robling et al. 2006).

In titanosaurs, the gross microstructure resembles that observed in nodosaurids—the high CoI is also accompanied by high vascularization (e.g., Cerda and Powell 2010; Cerda et al. 2015). However, the vascularization pattern is distinct from that of nodosaurids, as titanosaurs have wide chambers and a main vascular canal running along the main axis of the osteoderm (Cerda and Powell 2010; Curry Rogers et al. 2011; Cerda et al. 2015; Vidal et al. 2017). Such vascularization in titanosaurs has led to the hypothesis that physiological balance/calcium remobilization is the primary role of osteoderms in this group (Curry-Rogers 2011; Vidal et al. 2017). We argue, however, that this morphology in titanosaurs is consistent with the trade-off between protection/calcium balance found in crocodiles throughout their ontogeny (Sun and Chen 2013; Chen et al. 2014; Clarac et al. 2019). Therefore, the similar degree of high vascularization and higher SI found in nodosaurids, suggests that, besides a role in body armoring, their body osteoderms would also have an important physiological balance role in calcium remobilization. This later physiological role is clear among the new CAV specimens from Antarctica and published images of other ankylosaurian osteoderms. High vascularization, resorption cavities, and high SI support the interpretation of the role of body osteoderms in calcium balance (Cerda et al. 2019: fig. 2A). This extremely important but previously overlooked physiological function of ankylosaurian osteoderms may well have played a key role as a preadaptation to extreme environmental conditions, such as those represented by the low light conditions and lower temperatures during the Cretaceous Antarctic winter.

Conclusions

Understanding the function and evolution of the unique body armor of ankylosaurian dinosaurs is still in its infancy and is highly limited by phylogenetic instability and low sample sizes from geographic regions in the Southern Hemisphere. We shed some light on those topics by describing new specimens recovered from Antarctica, combining their data with previous data, and assessing the evolution of

osteoderms across morphospace and evolutionary history based on an updated phylogenetic hypothesis.

Our results indicate that it is possible to use osteoderms to differentiate between ankylosaurid and nodosaurid osteoderms based on their microstructures. However, we could not differentiate ankylosaurian osteoderms from those of titanosaurs. The newly discovered Antarctic material (CAV specimens) share a microstructural pattern with late-diverging nodosaurids and are recovered phylogenetically within this group. Additionally, all CAVs share the highly ordered arrangement of the structural fibers in the superficial cortex with the parankylosaurian *Antarctopelta* and the late-diverging nodosaurid *Sauropelta* (Fig. 9B). Finally, CAVs possess a histological microstructure pattern compatible with an early ontogenetic stage.

We provide quantitative support for previous hypotheses that ankylosaurids share the microstructure and the morphospace of early-diverging nodosaurids—previously recognized as “polacanthids” (Burns and Currie 2014). Late-diverging nodosaurids are very distinct from all other ankylosaurians by their thin or absent basal cortex and thick core. Such osteoderm structure is similar to that observed in the osteoderms of titanosaurs that lack wide chambers and/or wide vascular networks, (e.g., *Saltasaurus*). As previously hypothesized, the primary function of osteoderms of both ankylosaurids and nodosaurids could be to act body armor. Additionally, we provide histological evidence combined with information from the literature that nodosaurids underwent a rapid early growth strategy combined with an increase of osteoderm vascularization, suggesting some role in calcium remobilization for physiological balance, as in titanosaur sauropods. Therefore, the function of body osteoderms in dinosaurs, especially in ankylosaurians, seems to be characterized by a more complex trade-off mechanism between biomechanical and physiological functions than simplistic explanations related to body protection or display, as previously thought, and the growth pattern in long bones of *Antarctopelta* indicate they were preadapted to the colonization of higher-latitude environments.

Acknowledgments

This project was supported by Programa Antártico Brasileiro (PROANTAR) through the Conselho Nacional de Desenvolvimento Científico e Tecnológico (CNPq; grant nos. 420687/2016-5 and 313461/2018-0 to A.W.A.K.; no. 314222/2020-0 to J.M.S.) and Coordenação de Aperfeiçoamento de Pessoal de Nível Superior (CAPES: PROANTAR fellowship no. 88887.336584/2019-00 to A.S.B.). A.W.A.K. acknowledges funding from Fundação de Desenvolvimento Carlos Chagas Filho de Amparo à Pesquisa do Estado do Rio de Janeiro (FAPERJ no. E-26/202.905/2018) and T.R.S. acknowledges a postdoctoral fellowship provided by the Natural Sciences and Engineering Research Council of Canada (NSERC). We thank T. M. Scheyer, T. G. Frauenfelder, an anonymous reviewer, and N. Campione for comments that helped improve the quality of the article. We acknowledge the Willi Henning Society for the free availability of the software TNT. The team of the PALEOANTAR Project thanks the entire NApOc Ary Rongel military group and the pilots of the HU-1 helicopter squadron for their logistic support during fieldwork on the Antarctic Peninsula.

Declaration of Competing Interests

The authors declare no competing interests.

Data Availability Statement

Data available from the Dryad Digital Repository: <https://doi.org/10.5061/dryad.ht76hdrkx>.

Literature Cited

- Arbour, V. M., and P. J. Currie. 2016. Systematics, phylogeny and palaeobiogeography of the ankylosaurid dinosaurs. *Journal of Systematic Palaeontology* 14:385–444.
- Arbour, V. M., L. E. Zanno, and T. Gates. 2016. Ankylosaurian dinosaur palaeoenvironmental associations were influenced by extirpation, sea-level fluctuation, and geodispersal. *Palaeogeography, Palaeoclimatology, Palaeoecology* 449:289–299.
- Bellardini, F., and I. A. Cerda. 2017. Bone histology sheds light on the nature of the “dermal armor” of the enigmatic sauropod dinosaur *Agustinia ligabuei* Bonaparte, 1999. *Science of Nature* 104:1.
- Broeckhoven, C., A. du Plessis, and C. Hui. 2017. Functional trade-off between strength and thermal capacity of dermal armor: insights from girdled lizards. *Journal of the Mechanical Behavior of Biomedical Materials* 74:189–194.

- Brown, C. M. 2017. An exceptionally preserved armored dinosaur reveals the morphology and allometry of osteoderms and their horny epidermal coverings. *PeerJ* 5:e4066.
- Brown, C. M., D. M. Henderson, J. Vinther, I. Fletcher, A. Sistiaga, J. Herrera, and R. E. Summons. 2017. An exceptionally preserved three-dimensional armored dinosaur reveals insights into coloration and cretaceous predator-prey dynamics. *Current Biology* 27:2514–2521.e3.
- Brum, A. S., T. R. Simões, G. A. Souza, A. E. P. Pinheiro, R. G. Figueiredo, M. W. Caldwell, J. M. Sayão, and A. W. A. Kellner. 2022. Ontogeny and evolution of the elasmosaurid neck highlight greater diversity of Antarctic plesiosaurs. *Palaeontology* 62(2):e12593.
- Brum, A. S., L. H. S. Eleutério, T. R. Simões, M. R. Whitney, G. A. Souza, J. M. Sayão, and A. W. A. Kellner. 2023. Data from: Ankylosaurian body armor function and evolution with insights from osteohistology and morphometrics of new specimens from the Late Cretaceous of Antarctica. Dryad, dataset. <https://doi.org/10.5061/dryad.ht76hdrkx>
- Burns, M. E. 2008. Taxonomic utility of ankylosaur (Dinosauria, Ornithischia) osteoderms: *Glyptodontopelta minus* Ford, 2000: a test case. *Journal of Vertebrate Paleontology* 28:1102–1109.
- Burns, M. E., and P. J. Currie. 2014. External and internal structure of ankylosaur (Dinosauria, Ornithischia) osteoderms and their systematic relevance. *Journal of Vertebrate Paleontology* 34:835–851.
- Burns, M. E., and R. M. Sullivan. 2011. A new ankylosaurid from the Upper Cretaceous Kirtland Formation, San Juan Basin, with comments on the diversity of ankylosaurids in New Mexico. *New Mexico Museum of Natural History and Science Bulletin* 53:169–178.
- Burns, M. E., P. J. Currie, R. L. Sissons, and V. M. Arbour. 2011. Juvenile specimens of *Pinacosaurus grangeri* Gilmore, 1933 (Ornithischia: Ankylosauria) from the Late Cretaceous of China, with comments on the specific taxonomy of *Pinacosaurus*. *Cretaceous Research* 32:174–186.
- Burton-Johnson, A., and T. R. Riley. 2015. Autochthonous v. accreted terrane development of continental margins: a revised in situ tectonic history of the Antarctic Peninsula. *Journal of the Geological Society, London* 172:822–835.
- Buss, D. M., M. G. Haselton, T. K. Shackelford, A. L. Bleske, and J. C. Wakefield. 1998. Adaptations, exaptations, and spandrels. *American Psychologist* 53:533–548.
- Cerda, I. A., and J. E. Powell. 2010. Dermal armor histology of *Saltasaurus loricatus*, an Upper Cretaceous sauropod dinosaur from Northwest Argentina. *Acta Palaeontologica Polonica* 55:389–398.
- Cerda, I. A., R. A. García, J. E. Powell, and O. Lopez. 2015. Morphology, microanatomy, and histology of titanosaur (Dinosauria, Sauropoda) osteoderms from the Upper Cretaceous of Patagonia. *Journal of Vertebrate Paleontology* 35:37–41.
- Cerda, I. A., Z. Gasparini, R. A. Coria, L. Salgado, M. Reguero, D. Ponce, R. Gonzalez, J. M. Jannello, and J. Moly. 2019. Paleobiological inferences for the Antarctic dinosaur *Antarctopelta oliveroi* (Ornithischia: Ankylosauria) based on bone histology of the holotype. *Cretaceous Research* 103:104171.
- Chen, I. H., W. Yang, and M. A. Meyers. 2014. Alligator osteoderms: mechanical behavior and hierarchical structure. *Materials Science and Engineering C* 35:441–448.
- Chinsamy, A. 2005. The microstructure of dinosaurs bone: deciphering biology with fine scale techniques. Johns Hopkins University Press, Baltimore.
- Chinsamy, A., and M. A. Raath. 1992. Preparation of fossil bone for histological examination. *Palaeontologia Africana* 29:39–44.
- Chinsamy, A., I. Cerda, and J. Powell. 2016. Vascularised endosteal bone tissue in armoured sauropod dinosaurs. *Scientific Reports* 6:24858.
- Clarac, F., F. Goussard, V. De Buffrénil, and V. Sansalone. 2019. The function(s) of bone ornamentation in the crocodylomorph osteoderms: a biomechanical model based on a finite element analysis. *Paleobiology* 45:182–200.
- Curry Rogers, K., M. D'Emic, R. Rogers, M. Vickaryous, and A. Cagan. 2011. Sauropod dinosaur osteoderms from the Late Cretaceous of Madagascar. *Nature Communications* 2:564.
- D'Emic, M. D., J. A. Wilson, and S. Chatterjee. 2009. The titanosaur (Dinosauria: Sauropoda) osteoderm record: review and first definitive specimen from India. *Journal of Vertebrate Paleontology* 29:165–177.
- Francillon-Vieillot, H., V. de Buffrénil, J. Castenet, J. Geraudie, F. J. Meunier, J.-Y. Sire, I. Zylberberg, and A. de Ricqlès. 1990. Microstructure and mineralization of vertebrate skeletal tissues. Pp. 471–548 in J. G. Carter, ed. *Skeletal biomineralization patterns, processes and evolutionary trends*. Van Nostrand Reinhold, New York.
- Frauenfelder, T. G., P. R. Bell, T. Brougham, J. J. Bevitt, R. D. C. Bicknell, B. P. Kear, S. Wroe, and N. E. Campione. 2022. New ankylosaurian cranial remains from the Lower Cretaceous (Upper Albian) Toolebuc Formation of Queensland, Australia. *Frontiers in Earth Science* 10:803505.
- Goloboff, P. A., and S. A. Catalano. 2016. TNT version 1.5 including full implementation of phylogenetic morphometrics. *Cladistics* 32:221–238.
- Gould, S. J. 1991. Exaptation: a crucial tool for an evolutionary psychology. *Journal of Social Issues* 47:43–65.
- Gould, S. J., and E. S. Vrba. 1982. Paleontological Society exaptation—a missing term in the science of form exaptation. *Paleobiology* 8:4–15.
- Haines, R. W., and A. Mohuiddin. 1968. Metaplastic bone. *Journal of Anatomy* 103:527–538.
- Hammer, Ø., D. A. T. Harper, and P. D. Ryan. 2001. PAST: paleontological statistics software package for education and data analysis. *Palaeontologia Electronica* 4.
- Hayashi, S., K. Carpenter, and D. Suzuki. 2009. Different growth patterns between the skeleton and osteoderms of *Stegosaurus* (Ornithischia: Thyreophora). *Journal of Vertebrate Paleontology* 29:123–131.
- Hayashi, S., K. Carpenter, T. M. Scheyer, M. Watabe, and D. Suzuki. 2010. Function and evolution of ankylosaur dermal armor. *Acta Palaeontologica Polonica* 55:213–228.
- Hill, R. V. 2005. Integration of morphological data sets for phylogenetic analysis of Amniota: the importance of integumentary characters and increase taxonomic sampling. *Systematic Biology* 54:530–547.
- Hill, R. V., L. M. Witmer, and M. A. Norell. 2003. A new specimen of *Pinacosaurus grangeri* (Dinosauria: Ornithischia) from the Late Cretaceous of Mongolia: ontogeny and phylogeny of ankylosaurians. *American Museum Novitates* 3395:1–29.
- Kellner, A. W. A. 2022. Research in Antarctica—challenging but necessary. *Anais da Academia Brasileira de Ciências* 94(Suppl. 1): e20229451.
- Kellner, A. W. A., T. R. Simões, D. Riff, O. Grillo, P. Romano, H. P. Silva, R. Ramos, M. Carvalho, J. M. Sayão, G. Oliveira, and T. Rodrigues. 2011. The oldest plesiosaur (Reptilia, Sauropterygia) from Antarctica. *Polar Research* 30:7265.
- Kellner, A. W. A., T. Rodrigues, F. R. Costa, L. C. Weinschütz, R. G. Figueiredo, G. A. Souza, A. S. Brum, L. H. S. Eleutério, C. W. Mueller, and J. M. Sayão. 2019. Pterodactylid pterosaur bones from Cretaceous deposits of the Antarctic Peninsula. *Anais da Academia Brasileira de Ciências* 91(Suppl. 2): e20191300.
- Kilmer, J. T., and R. L. Rodríguez. 2017. Ordinary least squares regression is indicated for studies of allometry. *Journal of Evolutionary Biology* 30:4–12.

- Kirkland, J. I., L. Alcalá, M. A. Loewen, E. Espílez, L. Mampel, and J. P. Wiersma. 2013. The basal nodosaurid ankylosaur *Europelta carbonensis* n. gen., n. sp. from the Lower Cretaceous (Lower Albian) Escucha Formation of Northeastern Spain. *PLoS ONE* 8:e80405.
- Lamanna, M. C., J. A. Case, E. M. Roberts, V. M. Arbour, R. C. Ely, S. W. Salisbury, J. A. Clarke, D. E. Malinzak, A. R. West, and P. M. O'Connor. 2019. Late Cretaceous non-avian dinosaurs from the James Ross Basin, Antarctica: description of new material, updated synthesis, biostratigraphy, and paleobiogeography. *Advances in Polar Science* 30:228–250.
- Lamm, E.-T. 2013. Preparation and sectioning of specimens. Pp. 55–160 in K. Padian and E.-T. Lamm, eds. *Bone histology of fossil tetrapods: advancing methods, analysis, and interpretation*. University of California Press, Berkeley.
- Levrat-Calviac, V., and L. Zylberberg. 1986. The structure of the osteoderms in the gekko: *Tarentola mauritanica*. *American Journal of Anatomy* 176:437–446.
- Lima, F. J., J. M. Sayão, L. C. M. O. Ponciano, L. C. Weinschütz, R. G. Figueiredo, T. Rodrigues, R. A. M. Bantim, A. F. Saraiva, A. Jasper, D. Uhl, and A. W. A. Kellner. 2021. Wildfires in the Campanian of James Ross Island: a new macro-charcoal record for the Antarctic Peninsula. *Polar Research* 40:5487.
- Loewen, M. A., M. E. Burns, M. A. Getty, J. I. Kirkland, and M. K. Vickaryous. 2013. Review of Late Cretaceous ankylosaurian dinosaurs from the Grand Staircase region, southern Utah. Pp. 445–462 in A. L. Titus and M. A. Loewen, eds. *At the top of the grand staircase: the Late Cretaceous of southern Utah*. Indiana University Press, Bloomington.
- Maidment, S. C. R., S. J. Strachan, D. Ouarhache, T. M. Scheyer, E. E. Brown, V. Fernandez, Z. Johanson, T. J. Raven, and P. M. Barrett. 2021. Bizarre dermal armour suggests the first African ankylosaur. *Nature Ecology and Evolution* 5:1576–1581.
- Main, R. P., A. de Ricqlès, J. R. Horner, and K. Padian. 2005. The evolution and function of thyreophoran dinosaur scutes: implications for plate function in stegosaurs. *Paleobiology* 31:291–314.
- Marsh, O. C. 1890. Additional characters of the Ceratopsidae, with notice of new Cretaceous dinosaurs. *American Journal of Science* 39:418–426.
- Nopsca, B. F. 1915. Die Dinosaurier der Siebenbürgischen landesteile Ungarns. *Mitteilungen aus den Jahrbuch der Königlich Ungarischen Geologischen Reichsanstalt* 23:1–24.
- O'Gorman, J. P., R. Otero, M. Reguero, and Z. Gasparini. 2019. Cretaceous Antarctic plesiosaurs: stratigraphy, systematics and paleobiogeography. *Advances in Polar Science* 30:210–227.
- Olivero, E. B. 2012a. New Campanian kossmaticeratid ammonites from the James Ross Basin, Antarctica, and their possible relationships with *Jimboiceras? antarcticum* Riccardi. *Revue de Paléobiologie Vol. spéc.* 11:133–149.
- Olivero, E. B. 2012b. Sedimentary cycles, ammonite diversity and palaeoenvironmental changes in the Upper Cretaceous Marambio Group, Antarctica. *Cretaceous Research* 34:348–366.
- Olivero, E. B., and F. A. Medina. 2000. Patterns of Late Cretaceous ammonite biogeography in southern high latitudes: the family Kossmaticeratidae in Antarctica. *Cretaceous Research* 21:269–279.
- Organ, C. L., and J. Adams. 2005. The histology of ossified tendon in dinosaurs. *Journal of Vertebrate Paleontology* 25:602–613.
- Osborn, H. F. 1923. Two Lower Cretaceous dinosaurs of Mongolia. *American Museum Novitates* 95:1–10.
- Owen, R. 1842. Report on British fossil reptiles—Part II. Report of the British Association for the Advancement of Science 11:60–204.
- Pinheiro, A. P., A. A. F. Saraiva, W. Santana, J. M. Sayão, R. G. Figueiredo, T. Rodrigues, L. C. Weinschütz, L. C. M. O. Ponciano, and A. W. A. Kellner. 2020. New Antarctic clawed lobster species (Crustacea: Decapoda: Nephropidae) from the Upper Cretaceous of James Ross Island. *Polar Research* 39. <https://doi.org/10.33265/polar.v39.3727>.
- Piovesan, E. K., O. J. Correia Filho, R. M. Melo, L. D. Lacerda, R. O. Dos Santos, A. P. Pinheiro, F. R. Costa, J. M. Sayão, and A. W. A. Kellner. 2021. The Campanian–Maastrichtian interval at the Naze, James Ross Island, Antarctica: microbiostratigraphic and paleoenvironmental study. *Cretaceous Research* 120:104725.
- Ponce, D. A., I. A. Cerda, J. B. Desojo, and S. J. Nesbitt. 2017. The osteoderm microstructure in doswelliids and proterochampsids and its implications for palaeobiology of stem archosaurs. *Acta Palaeontologica Polonica* 62:819–831.
- Reguero, M. A., Z. Gasparini, E. B. Olivero, R. A. Coria, M. S. Fernández, J. P. O'Gorman, S. Gouiric-Cavalli, C. A. Hospitaleche, P. Bona, A. Iglesias, J. N. Gelfo, M. E. Raffi, J. J. Moly, S. N. Santillana, and M. Cárdenas. 2022. Late Campanian–Early Maastrichtian vertebrates from the James Ross Basin, West Antarctica, and paleobiogeography. *Anais da Academia Brasileira de Ciências* 94(Suppl. 1):e20211142.
- Ricqlès, A. J. de, X. Pereda Suberbiola, Z. Gasparini, and E. Olivero. 2001. Histology of dermal ossifications in an ankylosaurian dinosaur from the Late Cretaceous of Antarctica. VII International Symposium on Mesozoic Terrestrial Ecosystems. *Asociación Paleontológica Argentina Publicación especial* 7(1):171–174.
- Rivera-Sylva, H. E., E. Frey, W. Stinnesbeck, G. Carbot-Chanona, I. E. Sanchez-Urbe, and R. Guzmán-Gutiérrez. 2018. Paleodiversity of Late Cretaceous Ankylosauria from Mexico and their phylogenetic significance. *Swiss Journal of Paleontology* 137:83–93.
- Robling, A. G., A. B. Castillo, and C. H. Turner. 2006. Biomechanical and molecular regulation of bone remodeling. *Annual Review of Biomedical Engineering* 8:455–498.
- Rozadilla, S., A. M. A. Rolando, M. J. Motta, and F. E. Novas. 2016. On the validity of the Antarctic ankylosaur *Antarctopelta oliveroi* Salgado & Gasparini (Dinosauria, Ornithischia). Pp. 37 in E. Board, ed. *Abstracts XXX Jornadas Argentinas de Paleontología de Vertebrados*. Ameghiniana 53(6) (R).
- Salgado, L. 2003. Considerations on the bony plates assigned to titanosaurs (Dinosauria, Sauropoda). *Ameghiniana* 40:441–456.
- Salgado, L., and Z. Gasparini. 2006. Reappraisal of an ankylosaurian dinosaur from the Upper Cretaceous of James Ross Island (Antarctica). *Geodiversitas* 28:119–135.
- Santos, A., E. K. Piovesan, J. Guzmán, C. D. Usman, L. C. Weinschütz, R. J. M. Santos, G. R. Oliveira, R. G. Figueiredo, J. H. Z. Ricetti, E. Wilner, J. M. Sayão, and A. W. A. Kellner. 2022. Paleoenvironment of the Cerro Negro Formation (Aptian, Early Cretaceous) of Snow Island, Antarctic Peninsula. *Anais da Academia Brasileira de Ciências* 94(Suppl. 1):e20201944.
- Scheyer, T. M., and M. P. Sander. 2004. Histology of ankylosaur osteoderms: implications for systematics and function. *Journal of Vertebrate Paleontology* 24:874–893.
- Scheyer, T. M., J. B. Desojo, and I. A. Cerda. 2014. Bone histology of phytosaur, aetosaur, and other archosauriform osteoderms (Eureptilia, Archosauromorpha). *Anatomical Record* 297:240–260.
- Schneider, C. A., W. S. Rasband, and K. W. Eliceiri. 2012. NIH Image to ImageJ: 25 years of image analysis. *Nature Methods* 9:671–675.
- Seeley, T. M. 1888. The classification of the Dinosauria. Report of the British Association for the Advancement of Science 1887:698–699.
- Soto-Acuña, S., A. O. Vargas, J. Kaluza, M. A. Lepepe, J. F. Botelho, J. Palma-Liberona, C. Simon-Gutstein, R. A. Fernández, H. Ortiz, V. Milla, B. Aravena, L. M. E. Manríquez, J. Alarcón-Muñoz, J. P. Pino, C. Trevisan, H. Mansilla, L. F. Hinojosa, V. Muñoz-Walther, and D. Rubilar-Rogers. 2021. Bizarre tail weaponry in a transitional ankylosaur from subantarctic Chile. *Nature* 600:259–263.
- Sun, C., and P. Chen. 2013. Structural design and mechanical behavior of alligator (*Alligator mississippiensis*) osteoderms. *Acta Biomaterialia* 9:9049–9064. <https://doi.org/10.1016/j.actbio.2013.07.016>
- Thompson, R. S., J. C. Parish, S. C. R. Maidment, and P. M. Barrett. 2012. Phylogeny of the ankylosaurian dinosaurs

- (Ornithischia: Thyreophora). *Journal of Systematic Palaeontology* 10:301–312.
- Vickaryous, M. K., and B. K. Hall. 2006. Osteoderm morphology and development in the nine-banded armadillo, *Dasypus novemcinctus* (Mammalia, Xenarthra, Cingulata). *Journal of Morphology* 267:1273–1283.
- Vickaryous, M. K., and B. K. Hall. 2008. Development of the dermal skeleton in *Alligator mississippiensis* (Archosauria, Crocodylia) with comments on the homology of osteoderms. *Journal of Morphology* 269:398–422.
- Vickaryous, M. K., and J. Sire. 2009. The integumentary skeleton of tetrapods: origin, evolution, and development. *Journal of Anatomy* 214:441–464.
- Vidal, D., F. Ortega, F. Gascó, A. Serrano-Martínez, and J. L. Sanz. 2017. The internal anatomy of titanosaur osteoderms from the Upper Cretaceous of Spain is compatible with a role in oogenesis. *Scientific Reports* 7:1–11.
- Videira-Santos, R., S. Scheffer, L. Ponciano, L. C. Weinschütz, R. G. Figueiredo, T. Rodrigues, J. M. Sayão, D. S. Riff, and A. W. A. Kellner. 2020. First description of scleractinian corals from the Santa Marta and Snow Hill Island (Gamma Member) formations, Upper Cretaceous, James Ross Island, Antarctica. *Advances in Polar Science* 31:205–214.
- Warton, D. I., I. J. Wright, D. S. Falster, and M. Westoby. 2006. Bivariate line-fitting methods for allometry. *Biological Reviews of the Cambridge Philosophical Society* 81:259–291.